Phenomenological Approach to Cancer Cell Persistence

David A. Kessler*
Department of Physics, Bar-Ilan University, Ramat-Gan 52900, Israel

Herbert Levine
Center for Theoretical Biological Physics and Departments of Physics and Bioengineering, Northeastern University, Boston, Massachusetts 02215, USA

(Received 4 April 2022; accepted 11 July 2022; published 29 August 2022)

Drug persistence is a phenomenon by which a small percentage of cancer cells survive the presentation of targeted therapy by transitioning to a quiescent state. Eventually some of these persister cells can transition back to an active growing state and give rise to resistant tumors. Here we introduce a quantitative genetics approach to drug-exposed populations of cancer cells in order to interpret recent experimental data regarding inheritance of persister probability. Our results indicate that alternating periods of drug treatment and drug removal may not be an effective strategy for eliminating persisters.

DOI: 10.1103/PhysRevLett.129.108101

Introduction.—One of the most significant problems facing the cancer community is that of the emergence of drug resistance to targeted therapies [1]. A typical scenario is that a drug will yield an immediate benefit, namely, reduction of tumor burden, for a significant percentage of those patients whose tumors have been classified as relying on driver mutations in a specific pathway targeted by the drug. Yet, after some relatively short time, tumor growth will rebound and the patient's condition will deteriorate. Understanding mechanisms enabling this resistance and thereby finding approaches to prevent its occurrence is clearly of the utmost importance.

Resistance mechanisms can involve genetic changes, phenotypic remodeling, or both [2]. One of the interesting discoveries during recent years has been the role of the phenomenon of persistence in enabling eventual resistance, wherein some tumor cells manage to survive for long periods of time even in the presence of drug concentrations that kill most cells [3]. Persistence was originally discovered in the context of small bacterial subpopulations able to withstand antibiotics [4,5]. In the cancer context, persisters have been seen, for example, in the response of PC9 lung cancer cells to Epidermal Growth Factor Receptor (EGFR) inhibitors [6]. Here, some cells will transition to a quiescent state with a diminished death rate. Eventually, some of these cells will regain the ability to grow [7] and may eventually fix mutations that confer complete resistance [8]. This basic phenomenology has been seen in a wide variety of different cancer contexts; see, e.g., Ref. [9]. Persistence in bacterial systems seems to rely on discrete subpopulations resulting from multistability in those genetic networks coupled to growth [10–12]. In cancer cells, conversely, persistence seems to be a quantitative trait that can vary continuously between specific clonal subpopulations.

In this Letter, we formulate a population-based model of cancer cell persistence. We are motivated by recent experimental work [13] indicating that individual cancer cells are characterized by a "chance to persist" (CTP) and survive a week of drug exposure. Clones produced from a single cell retain this trait, so that those cells that survive have, on average, a larger chance to persist, and thus there is long-term populational memory of previous drug treatment. Interestingly, clones with differing values of CTP, when exposed to the drug, exhibit different rates of decay of their population levels beyond the one week mark (see below), suggesting a nontrivial coupling between the process that determines this percentage and cell death dynamics. Our model focuses on a mutation-selection approach [14,15] to the distribution of CTP and introduces an auxiliary survival variable whose dynamics governs how the decay rate of the population size in the presence of a specific drug depends on this CTP. We show that the timescale of return to this homeostatic persister distribution may be long enough to allow for drug-induced changes to the CTP distribution in the population to last for significant periods of time. All told, our framework quantifies persister behavior in terms of a small number of phenomenological parameters and hence provides a guidepost for interpreting data and investigating underlying molecular mechanisms.

Modeling approach.—Our model consists of two dynamical pieces, the first of which deals with the chance to persist. As shown in Berger *et al.* [13], one can operationally define a continuous variable called the chance to persist (CTP $\equiv x$) as the fraction of cells that have survived nominally lethal drug treatment over some fixed time τ, day 7 in the PC9 experiments. We assume that the homeostatic distribution of this trait is given by mutation-selection equilibrium with a penalty for higher CTP.

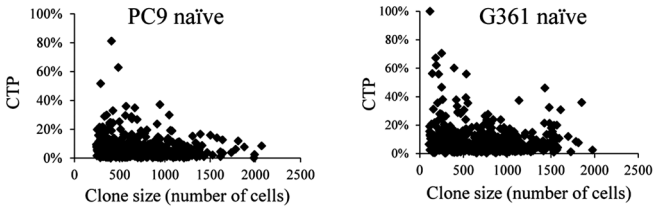

FIG. 1. CTP versus number of cells for a three week clonal expansion for two different persisting systems. Data show clearly that high CTP correlates with low net growth rate. From [13], courtesy of Nature Publishing Group.

In support of this, we note that measurement of clonal size after expansion for three weeks, shown in Fig. 1, depends inversely on CTP. Note that the term "mutation" here does not necessarily refer to an actual genomic change but could refer to an altered epigenetic state that is heritable [16]. The simplest such model takes the form, assuming an overall constant population size,

$$\frac{\partial P_X(x,t)}{\partial t} = -a(x-\bar{x}))P_X + \mu\frac{\partial^2 P_X}{\partial x^2}, \tag{1}$$

where μ is the rate of mutation and a is the birth rate penalty for having a CTP of unity. $\bar{x}$ is the instantaneous mean of the distribution, $\bar{x} \equiv \int dx\, x P_X(x,t)$, and the presence of this term guarantees the overall population size remains constant in time. We can rescale time to arrive at a one-parameter model depending on $\tilde{a} = a/\mu$. The steady-state solution of this system is given approximately (ignoring the range limitation on x) in terms of an Airy function

$$P_X^{ss} \sim \mathrm{Ai}[\tilde{a}^{1/3}(x-\bar{x})], \tag{2}$$

which is a strongly peaked function for large $\tilde{a}$, demonstrating the likelihood that most cells have a CTP within a small range of the average (low) CTP and hence only a small percentage of cells have a significant chance of persisting. In the Supplemental Material [17], we show that one can alternatively formulate a microscopic "agent-based" approach that leads to the same conclusion. A comparison of this predicted function to data from the aforementioned experiment is presented in Fig. 2. Later on, we will discuss how to estimate μ so as to determine the rate of relaxation back to the steady-state solution from a perturbed initial condition.

At a fixed value of CTP, i.e., in a clonal population originating from a single cell with some specific CTP and before mutation has had a chance to act, the experiment indicates that there is still significant phenotypic heterogeneity. This is inherent in the fact that CTP is a probability, i.e., the *chance* to persist. We introduce a new fluctuating variable s to capture this heterogeneity. In reality, we expect that s is a projection of the phenotypic degrees of freedom onto the one-dimensional axis related to succumbing to drug-induced death. If s is less than zero, cells die quickly

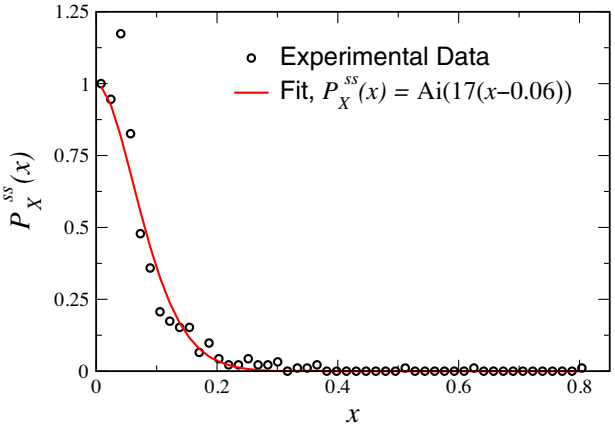

FIG. 2. Experimental data, courtesy of the Straussman group, for the distribution of CTP, together with a fit to $P_X^{ss}(x)$ versus x, from Eq. (2), yielding $\tilde{a}^{1/3} = 17$, $\bar{x} = 0.06$. Both distributions have been normalized to $P_X(0) = 1$.

with rate k. For a single cell, s changes stochastically as the cell's phenotype is buffeted by inherent fluctuations. The value of CTP x sets the equilibrium point $s_0(x)$, about which s fluctuates in the absence of the drug. Again opting for the simplest approach that captures our conceptual idea, we assume a modified Ornstein-Uhlenbeck (OU) process for the stochastic dynamics of s,

$$\frac{\partial P_S(s,t;x)}{\partial t} = b\frac{\partial}{\partial s}\{[s-s_0(x)]P_S\} + \sigma^2\frac{\partial^2 P_S}{\partial s^2} - \theta(-s)kP_S, \tag{3}$$

where $P_S(s,t;x)$ is the probability density of the surviving cells of the fixed-x clone with instantaneous phenotype s. The constant b represents the degree of selective pressure favoring s_0. σ^2 controls the size of the fluctuations in s. k is the death rate of cells with $s < 0$. Clearly, $s_0 < 0$ for low values of x, since then the typical cell does not survive its exposure to the drug. Using the operational definition of CTP, we can determine $s_0(x)$ by the relationship

$$\int_{-\infty}^{\infty} \mathrm{d}s\, P_S(s,\tau;x) = x, \tag{4}$$

where we start the population at $t = 0$ at the drug-free steady-state solution

$$P_S(s,0;x) = P_S^{ss}(s;x) = \frac{1}{\sqrt{2\pi\sigma^2/b}}\exp\left[\frac{-b[s-s_0(x)]^2}{2\sigma^2}\right].$$

A comparison of $s_0(x)$ with an approximation valid for small τ and large k with $k\tau \gg 1$, namely,

$$\int_{-\infty}^{0} \mathrm{d}s\, P_S^{ss}(s;x) = 1 - x \tag{5}$$

is presented in the Supplemental Material, Fig. S1 [17].

Population decay.—Given the model for the stochastic dynamics of s, we can compute population decline over

time, both for individual fixed-x clones and for the population as a whole. Since the units of s are arbitrary, we are free to set $\sigma^2 = b$, so that P_S^{ss} has unit variance. This leaves us with two timescales for the s dynamics, a fast one set by k and a slower one set by b. For a fixed x, the decay is asymptotically a single exponential. There is a simple way of showing this for the admittedly extreme case of $s_0 = 0$, $k \to \infty$. For this case, exactly half the cells die immediately upon entering drug treatment and the model reduces to the OU equation with an absorbing boundary at $s = 0$. This can be solved by the method of images, giving for positive s

$$P_S(s,t) = \int_o^\infty G(s,s';t,0)P_S^{ss}(s')\mathrm{d}s', \tag{6}$$

where G is Green's function for the OU equation with the boundary condition $G(s,s';t,0) = 0$ at $s = 0$,

$$G(s,s';t,0) = \frac{1}{\sqrt{2\pi(1-e^{-2bt})}}\left(e^{\frac{-(s-s'e^{-bt})^2}{(1-e^{-2bt})}} - e^{\frac{-(s+s'e^{-bt})^2}{(1-e^{-2bt})}}\right).$$

For large t one can expand in the object $s'e^{-bt}$ to obtain

$$P_S(s, t\to\infty) \sim ce^{-bt}sP_S^{ss}(s), \tag{7}$$

with $c = \int_0^\infty 2s'P_S^{ss}(s')$. Note the decay at rate b, the slow timescale. Going to finite k would decrease this rate, as it now takes additional time to die for cells entering the nonsurviving zone. On the other hand, going to the more relevant negative values of s_0 increases the rate, as attraction to the mean phenotype would accelerate the flux toward negative s.

To address the asymptotic decay rate at general parameter values, we can turn to an eigenvalue approach. Assuming that $P \sim e^{-\lambda t}$ leads to the following system:

$$-\lambda P_S = b\left\{\frac{\partial}{\partial s}[(s-s_0)P_S] + \frac{\partial^2 P_S}{\partial s^2}\right\} \qquad s > 0,$$
$$(k-\lambda)P_S = b\left\{\frac{\partial}{\partial s}[(s-s_0)P_S] + \frac{\partial^2 P_S}{\partial s^2}\right\} \qquad s < 0,$$

with continuity conditions on P and P' across $s = 0$. Writing $P \equiv \psi e^{-[(s-s_0)^2/4]}$ leads to a set of coupled parabolic cylinder equations for ψ, and one can easily derive the eigenvalue condition

$$\frac{D'_{\lambda/b}(-s_0)}{D_{\lambda/b}(-s_0)} = -\frac{D'_{(\lambda-k)/b}(s_0)}{D_{(\lambda-k)/b}(s_0)}, \tag{8}$$

where D is the parabolic cylinder function [18]. The resulting graph of $\lambda(s_0)$ is shown in the Supplemental Material, Fig. S2 [17]. One can verify that the resulting λ agrees with the long-time decay rate obtained from direct numerical solutions of the full equations, thereby confirming that the decay always transitions to pure exponential for long times.

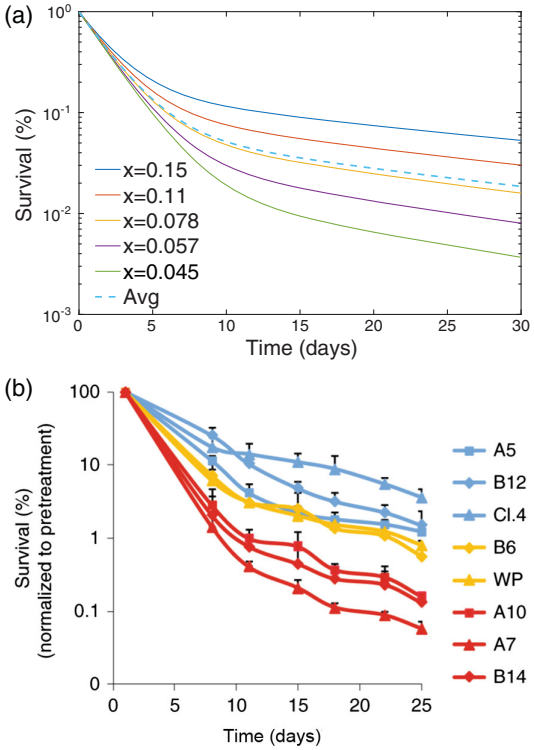

FIG. 3. (a) The decay of the population of various fixed-x clones, as well as for the entire population initially described by the steady-state x distribution, Eq. (2). Here $b = 0.03/\mathrm{day}$ and $k = 1/\mathrm{day}$. (b) The experimental results for the decay of various fixed-x clones (from Ref. [13], courtesy of Nature Publishing Group).

In Fig. 3(a), we show the decay plots for different specific values of the CTP. We see clearly the two timescales. This is reflected as well in the experimental data, shown for comparison in Fig. 3(b). The values of the rates b and k in the simulation were chosen to reproduce the experimental timescales, with $b = 0.03/\mathrm{day}$ and $k = 1/\mathrm{day}$. We show as well in Fig. 3 the decay for the entire population obtained by averaging over the CTP distribution given in Eq. (2). Since the CTP distribution is highly peaked, the global decay follows rather closely that of a typical CTP value. Note that the decay rate increases as CTP is lowered, as already mentioned above. This feature is also prominent in the experimental data in Fig. 3(b). Note that the model has the same k for different clones and hence all slopes start out the same. The first data point in Fig. 3(b) is at day 7 and hence no information is available about the validity of this assumption. Again, similar findings arise in our agent-based formulation discussed in the Supplemental Material [17].

Given the above, it is clear that the population structure will evolve as clones with low CTP preferentially die off. In Fig. 4, we show a sequence of population snapshots,

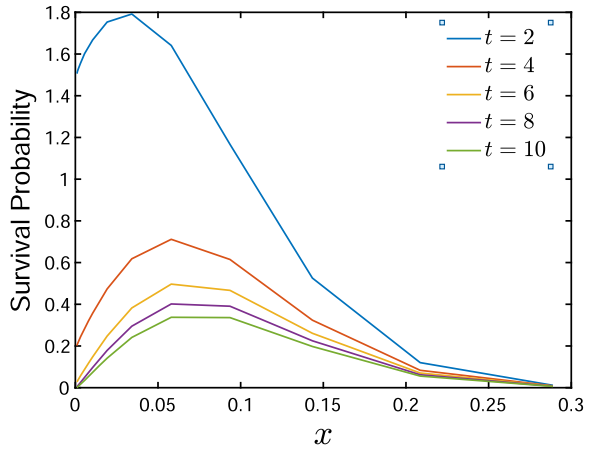

FIG. 4. The density of survivors as a function of x for various times, measured in days, starting from the steady-state x distribution, given by Eq. (2).

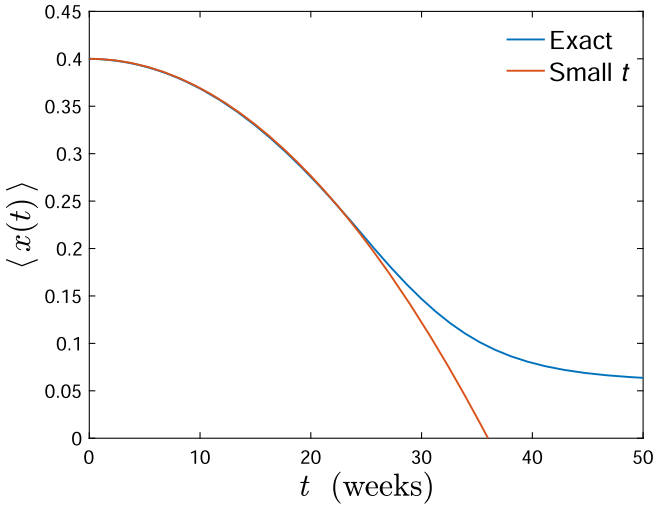

FIG. 5. $\langle x(t)\rangle$ versus t for the case of an initial clone with $x = 0.4$. $\mu = 2.5 \times 10^{-4}$/week, $a = 1.25$/week, and $\bar{x} = 0.06$.

assuming that the rate of mutational change is much slower than the rate of drug-induced selection. Finally, we note that the relatively slow timescale for survivability evolution will manifest itself in differences in measured properties of individual cells grown into subclones. These variations are relatively small and shorter lasting than the variations between clones. The presence of this variation in the experimental data of Ref. [13] does, however, lend general support to our notion of phenotypic variation both between clones and within the clonal population.

Clonal stability.—As discussed above, we have assumed that the nonclonal wild-type population arises as the steady-state of a mutation-selection process. This means that a clonal population will eventually revert to the original population from which it was drawn. Experimentally, this appears to take a considerable amount of time. In the experiments of Ref. [13], the CTP of individual clones seemed relatively stable for 18 weeks of temporal evolution in the absence of drug. In our model as given by Eq. (1), the rate at which changes occur that act to push the distribution back to its steady-state form is determined by the parameter μ. Solving for short times, starting from a single clone, we obtain

$$\frac{d\langle x\rangle}{dt} \simeq -a\mathrm{Var}[x] \simeq -\tilde{a}\mu\mathrm{Var}[x], \qquad \frac{d\mathrm{Var}[x]}{dt} \simeq 2\mu, \quad (9)$$

which immediately yields $\langle x\rangle = x_0 - \tilde{a}(\mu t)^2$. A comparison of this early-time prediction versus a full numerical integration of the governing equation is presented in Fig. 5, for a typical set of parameters. In order to compare this to the aforementioned experimental result, we need an estimate of μ. Given the above, evolving a clone for T days in the absence of drug would allow an estimate $\mu \sim (\mathrm{Var}[x]/2T)$. Based on the fact that there appears to be no significant change in the behavior of a single clone even after letting it evolve for 18 weeks means that $\tilde{a}(18\mu)^2$ is still small compared to a significant change in CTP (say, by an amount 0.1), which translates to

$$\tilde{a}(18\mu)^2 < 0.1. \quad (10)$$

Using the fit in Fig. 1 to determine $\tilde{a}$ and converting to percentage for measuring CTP gives μ smaller than 2.5×10^{-4}/week.

Discussion.—We have introduced a simple model to integrate data concerning clonal variability of the probability of persisting and the correlated rate of dying for cancer cells exposed to doses of targeted therapies. Our approach makes semiquantitative sense of the data from a recent experiment and offers new insights into the persistence phenomenon. It should therefore prove useful in the search for new approaches to prevent persistence from transitioning to complete resistance, thereby defeating drug efficacy. One conclusion that is already clear is that the simplest strategies of presenting drug intermittently [19] and thereby restoring drug sensitivity during the "holidays" have not taken into account the fact that these protocols will rapidly select for populations with higher persistence, which is retained due to the CTP memory.

One key assumption of our model is that the population distribution of the chance to persist, clearly peaked at low percentages, is determined by a growth penalty for persistence. This penalty is directly visible in Fig. 1, where clones at smaller CTP tend to grow larger over a three week period, but was much harder to detect in a 24 h growth assay [13]. We feel that an assay lasting for a time significantly shorter than the doubling time is likely to be more subject to systematic bias. We do note that the data at small CTP are rather noisy and hence one might imagine an extension of our basic population equation that takes

into account this stochasticity. We also note that the claim in [13] that there is no observed connection between some type of quiescence manifesting itself as a slower growth rate and the phenomenon of persistence, as indeed had been suggested in earlier work [20], is premature.

This Letter does not address the prospect of persister cells regaining growth, presumably by adapting their physiology to deal with the drug-induced stress. It is, of course, an interesting question to consider the extent to which a cell's survival value might influence its ability to transition back to growth. Given recent progress [7] in identifying phenotypic changes (especially related to cell metabolism) that correlate with the ability to resume cycling, this could be investigated in future experiments and in extensions of the current model.

D. A. K. acknowledges the support of the U.S.-Israel Binational Science Foundation, Grant No. 2015619. H. L. acknowledges the support of the NSF, Grants No. PHY-1935762 and No. PHY-2019745. We acknowledge useful conversations with Ravid Sraussman and Adi Berger.

*Corresponding author.
David.Kessler@biu.ac.il

[1] S. Boumahdi and F. J. de Sauvage, The great escape: Tumour cell plasticity in resistance to targeted therapy, Nat. Rev. Drug Discov. **19**, 39 (2020).
[2] R. Salgia and P. Kulkarni, The genetic/non-genetic duality of drug 'resistance' in cancer, Trends Cancer **4**, 110 (2018).
[3] S. V. Sharma, D. Y. Lee, B. Li, M. P. Quinlan, F. Takahashi, S. Maheswaran, U. McDermott, N. Azizian, L. Zou, M. A. Fischbach *et al.*, A chromatin-mediated reversible drug-tolerant state in cancer cell subpopulations, Cell **141**, 69 (2010).
[4] E. Chain, E. Duthie *et al.*, Bactericidal and bacteriolytic action of penicillin on the staphylococcus, Lancet **245**, 652 (1945).10.1016/S0140-6736(45)90042-0
[5] N. Q. Balaban, J. Merrin, R. Chait, L. Kowalik, and S. Leibler, Bacterial persistence as a phenotypic switch, Science **305**, 1622 (2004).
[6] A. N. Hata, M. J. Niederst, H. L. Archibald, M. Gomez-Caraballo, F. M. Siddiqui, H. E. Mulvey, Y. E. Maruvka, F. Ji, H.-e. C. Bhang, V. Krishnamurthy Radhakrishna *et al.*, Tumor cells can follow distinct evolutionary paths to become resistant to epidermal growth factor receptor inhibition, Nat. Med. **22**, 262 (2016).
[7] Y. Oren, M. Tsabar, M. S. Cuoco, L. Amir-Zilberstein, H. F. Cabanos, J.-C. Hütter, B. Hu, P. I. Thakore, M. Tabaka, C. P. Fulco *et al.*, Cycling cancer persister cells arise from lineages with distinct programs, Nature (London) **596**, 576 (2021).
[8] M. Ramirez, S. Rajaram, R. J. Steininger, D. Osipchuk, M. A. Roth, L. S. Morinishi, L. Evans, W. Ji, C.-H. Hsu, K. Thurley *et al.*, Diverse drug-resistance mechanisms can emerge from drug-tolerant cancer persister cells, Nat. Commun. **7**, 10690 (2016).
[9] C. A. Chang, J. Jen, S. Jiang, A. Sayad, A. S. Mer, K. R. Brown, A. M. Nixon, A. Dhabaria, K. H. Tang, D. Venet *et al.*, Ontogeny and vulnerabilities of drug-tolerant persisters in HER2+ breast cancer, Cancer Discov. **12**, 1022 (2022).
[10] E. Rotem, A. Loinger, I. Ronin, I. Levin-Reisman, C. Gabay, N. Shoresh, O. Biham, and N. Q. Balaban, Regulation of phenotypic variability by a threshold-based mechanism underlies bacterial persistence, Proc. Natl. Acad. Sci. U.S.A. **107**, 12541 (2010).
[11] J. Feng, D. A. Kessler, E. Ben-Jacob, and H. Levine, Growth feedback as a basis for persister bistability, Proc. Natl. Acad. Sci. U.S.A. **111**, 544 (2014).
[12] R. A. Fasani and M. A. Savageau, Molecular mechanisms of multiple toxin–antitoxin systems are coordinated to govern the persister phenotype, Proc. Natl. Acad. Sci. U.S.A. **110**, E2528 (2013).
[13] A. Jacob Berger, E. Gigi, L. Kupershmidt, Z. Meir, N. Gavert, Y. Zwang, A. Prior, S. Gilad, U. Harush, I. Haviv *et al.*, IRS1 phosphorylation underlies the non-stochastic probability of cancer cells to persist during EGRF inhibition therapy, Nat. Cancer **2**, 1055 (2021).
[14] T. B. Kepler and A. S. Perelson, Modeling and optimization of populations subject to time-dependent mutation, Proc. Natl. Acad. Sci. U.S.A. **92**, 8219 (1995).
[15] L. S. Tsimring, H. Levine, and D. A. Kessler, RNA Virus Evolution via a Fitness-Space Model, Phys. Rev. Lett. **76**, 4440 (1996).
[16] S. H. Sandholtz, Q. MacPherson, and A. J. Spakowitz, Physical modeling of the heritability and maintenance of epigenetic modifications, Proc. Natl. Acad. Sci. U.S.A. **117**, 20423 (2020).
[17] See Supplemental Material at http://link.aps.org/supplemental/10.1103/PhysRevLett.129.108101 for graphs of $s_0(x)$ and $\lambda(s_0)$, as well as a description of an agent-based modeling approach.
[18] M. Abramowitz and I. A. Stegun, *Handbook of Mathematical Functions with Formulas, Graphs, and Mathematical Tables* (US Government Printing Office, Washington, DC, 1964), Vol. 55.
[19] A. J. Kavran, S. A. Stuart, K. R. Hayashi, J. M. Basken, B. J. Brandhuber, and N. G. Ahn, Intermittent treatment of $BRAF^{V600E}$ melanoma cells delays resistance by adaptive resensitization to drug rechallenge, Proc. Natl. Acad. Sci. U.S.A. **119**, e2113535119 (2022).
[20] B. B. Paudel, L. A. Harris, K. N. Hardeman, A. A. Abugable, C. E. Hayford, D. R. Tyson, and V. Quaranta, A nonquiescent "idling" population state in drug-treated, BRAF-mutated melanoma, Biophys. J. **114**, 1499 (2018).